



# Photon Reconstruction Study for run2 Based on xAOD

Cong PENG

University of Chinese Academy of Sciences, Beijing

*Supervisor: Yanping HUANG*

September 11, 2014

## **Abstract**

From run 1 to run 2 in LHC, there are much change in software, detector configuration and analysis model(from DPD to xAOD), so we must make sure the photon reconstruction will be working well for photons with large transverse momentum in the final state are distinguishing signatures for many physics analyses at the LHC by the ATLAS experiment, such as the Standard Model measurement, or the search for more exotic particles such as the graviton and Super Summetry(SUSY) particles.

# Contents

<b>1</b>	<b>Introduction</b>	<b>3</b>
1.1	The ATLAS detector . . . . .	3
1.2	The ATLAS analysis framework evolution . . . . .	3
1.3	Theory . . . . .	4
<b>2</b>	<b>Measurement and analysis</b>	<b>4</b>
2.1	Photon Reconstruction Efficiency . . . . .	5
2.2	The performance of the single photon sample @ xAOD . . . . .	8
2.2.1	Separate the conversion type . . . . .	8
2.2.2	Separate the detector region . . . . .	9
2.2.3	Separate the reconstruction process . . . . .	10
2.3	Latest xAOD reco efficiency results . . . . .	12
<b>3</b>	<b>Conclusions</b>	<b>13</b>
<b>4</b>	<b>Acknowledgements</b>	<b>13</b>

# 1 Introduction

Photons with large transverse momentum in the final state are distinguishing signatures for many physics analyses at the LHC by the ATLAS experiment, such as the Standard Model measurement, or the search for more exotic particles such as the graviton and Super Symmetry(SUSY) particles and so on[1].

## 1.1 The ATLAS detector

The ATLAS inner detector(ID) provides precise track reconstruction over  $|\eta| \leq 2.5$ . It consists of three layers of pixel detectors close to the beam pipe, four layers of silicon microstrip detectors(SCT)providing eight hits per track at intermediate radii, and a transition radiation tracker(TRT) at the outer radii, providing about 30 hits per track(in the range  $|\eta| \leq 2.0$ ). The TRT also provides substantial discriminating power between electrons and pions over the wide energy range between 0.5 and 100GeV by utilizing transition radiation(TR)in polypropylene foils and fibres. The innermost pixel layer(also called the B-layer) is located (just outside the beam pipe)at a radius of 50mm, and provides precision vertexing.

The ATLAS electromagnetic(EM)calorimeter has a fine segmentation in both the lateral( $\eta \times \phi$  space)and longitudinal directions of the showers. At high energy, most of the EM shower energy is collected in the second layer which has a lateral granularity of  $0.025 \times 0.025$  in  $\eta \times \phi$  space. The first layer consists of finer-grained strips in the  $\eta$ -direction(with a coarser granularity in  $\phi$ ).These two layers are complemented by a presampler layer with coarse granularity placed in front to correct for energy lost in the material before the calorimeter, and by a back layer behind[3].

## 1.2 The ATLAS analysis framework evolution

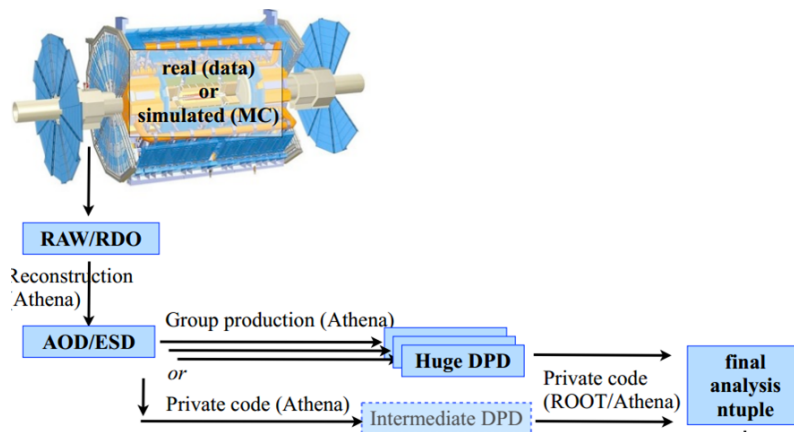


Figure 1: The analysis frameworks for run 1

In run 1 at LHC, there are actually two frameworks dedicated for the final physics analysis, one is for the AOD/ESD datasets and the other one is for the DPD datasets.

These cumbersome frameworks waste lots of storage space for large DPDs and production DPDs time and man power. The DPDs are actually only the copies of the AOD/ESD which are readable by Root. During this upgrade period from run 1 to run 2, we also upgrade the analysis model for run2 by combining the AOD/ESD and DPDs to a new format xAOD, the xAOD has the advantages that it is readable by both Athena and Root and most importantly it can be much more fast produced centrally and compact compared with DPDs.

### 1.3 Theory

The photons which are relevant to physics measurements will have energies in excess of 1 GeV. These photons must pass through the ATLAS tracker before depositing their energy in the EM calorimeter. At photon energies above 1 GeV, the interaction of photons with the tracker will be completely dominated by  $e^+e^-$  pair production in the presence of the material in Figure 2 and Figure 3 or Dalitz decay without material  $\gamma^* \rightarrow e^+e^-$ , such as Compton or Rayleigh scattering, will have cross-sections which are orders of magnitude below that for the photon conversion, and may thus be safely ignored. These truth level converted photons (defined as the conversion radius less than 800 mm) can be reconstructed as unconverted photons, 1-track conversion photons and 2-track conversion photons[2].

1-track conversion photon: for either track has low pt or the energy of the photon is very large that the we can not distinguish these tracks.

- 1Si track conversion: track has Si hits
- 1TRT track conversion: track is stand-alone TRT track

2-track conversion photon:

- 2SiSi tracks conversion :pairs in which both tracks have Si hits
- 2SiTRT tracks conversion :pairs in which one of the two tracks has Si hits
- 2TRTTRT tracks conversion :pairs in which both tracks are stand-alone tracks

The reconstruction of photons follows in its main aspects that of electrons, both objects are treated similarly within an overall reconstruction algorithm. There is an underlying similarity between electrons and converted photons due to the presence of the tracks in both objects, this results in a certain amount of mis reco electrons which are actually photons at truth level[1].

## 2 Measurement and analysis

The photon reconstruction efficiency between the DPD and xAOD, the performance of the single photon sample based on xAOD and latest xAOD reconstruction efficiency results are shown in the following parts:

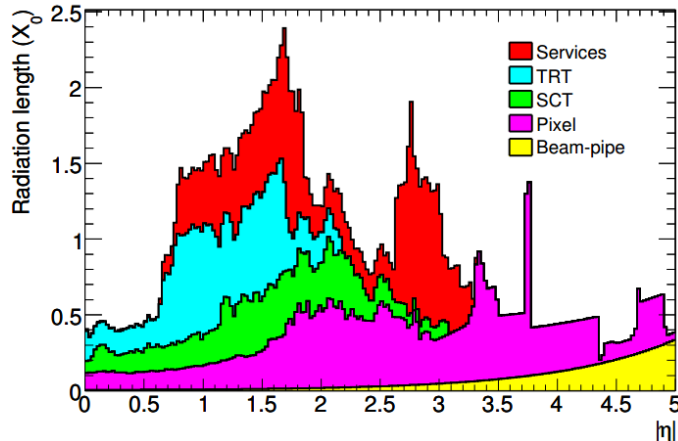


Figure 2: Material in the inner detector as a function of  $\eta$

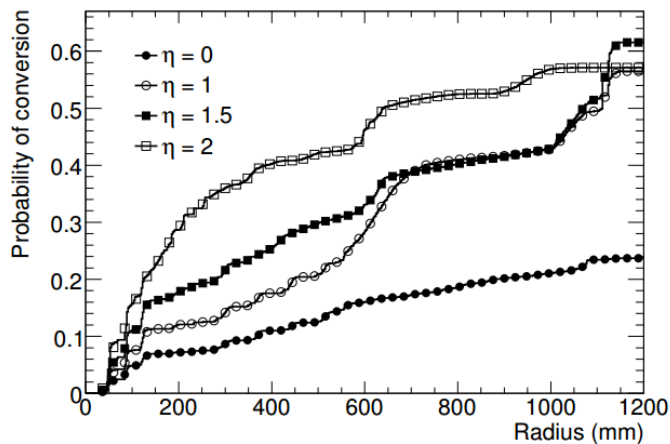


Figure 3: Probability of a photon to have converted as a function of radius for different values of pseudorapidity.

## 2.1 Photon Reconstruction Efficiency

Photons from  $H \rightarrow \gamma\gamma$  decays for  $m_H=125\text{GeV}$  with true transverse momentum  $p_T \geq 10\text{GeV}$  are used to compute the reconstruction efficiencies. The acceptance is limited to  $\|\eta\| \leq 2.37$ ,  $\eta$  being the true pseudorapidity position of the photon, and photons in the transition region between the barrel and end-cap cryostats ( $1.37 \leq \|\eta\| \leq 1.52$ ) are removed[1]. In Figure 4 the reconstruction efficiency for all photons (author=4,16) and original photons (author=4) are shown: the reconstruction efficiency for all photons in DPD is 96% while for the xAOD this efficiency is 89%, the reco efficiency for original photons in DPD is 59% while for the xAOD this efficiency is 79%. We also try to give the mis-electron reconstruction efficiency (truth photons but reco as electrons).

Figure 5 shows the overall reconstruction efficiency as a function of true  $\eta$ . In Figure 6, we further separate the reco efficiency of all photons to unconverted photons and converted photons. The reco efficiency for unconverted photons in xAOD is 100% which is consistent with the DPD, however, for converted photons in xAOD, the reco efficiency is 77% which is lower than DPD of 90%.

Figure 7 shows the reconstruction efficiency as a function of true  $\eta$

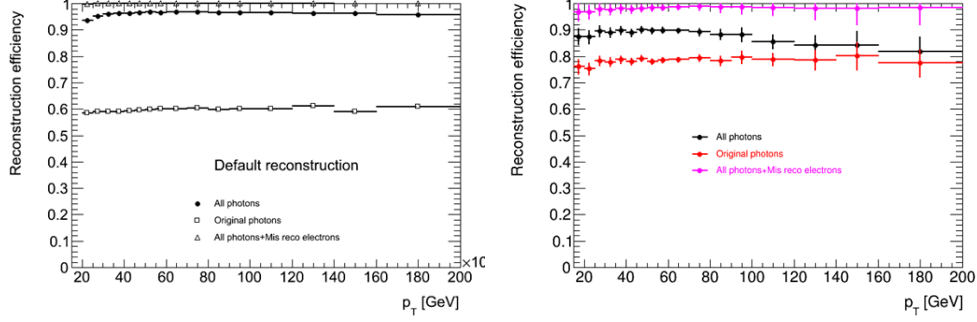


Figure 4: Overall photon reconstruction efficiencies as a function of true  $p_T$  (with acceptance cut: exclude:  $|\eta|$  in  $[1.37, 1.52]$ )

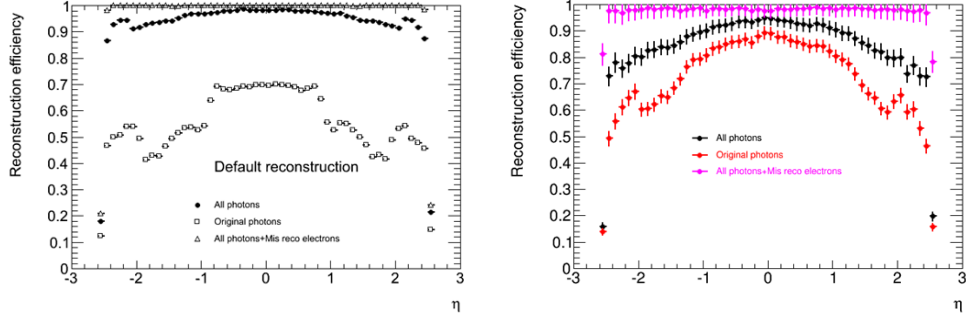


Figure 5: Overall photon reconstruction efficiencies as a function of true  $\eta$  (without acceptance cut)

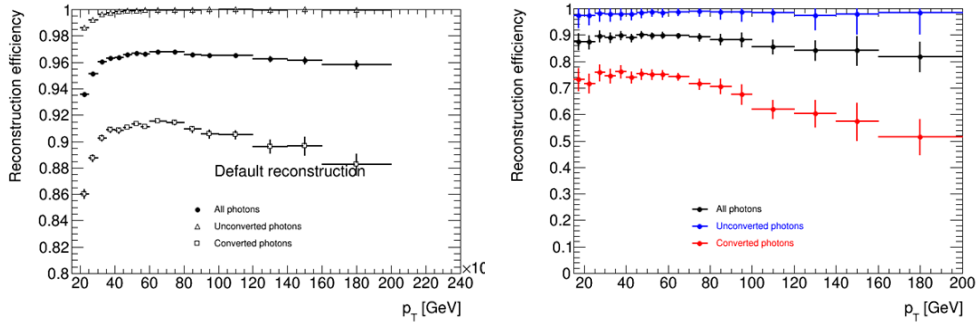


Figure 6: Photon reconstruction efficiencies as a function of true  $p_T$  (with acceptance cut) for unconverted and converted photons separately.

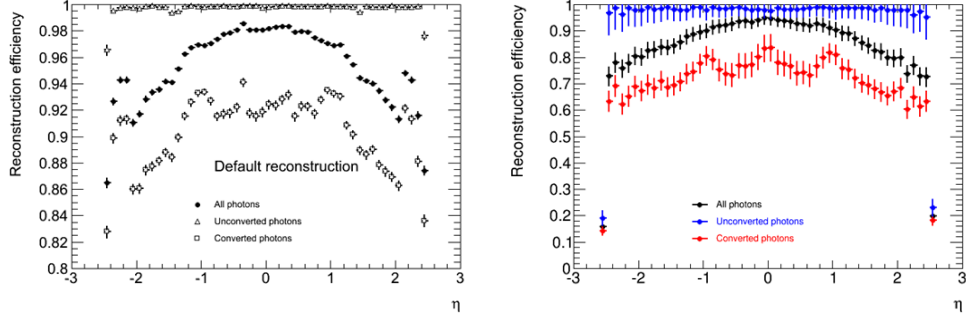


Figure 7: Photon reconstruction efficiencies as a function of true  $\eta$ (without acceptance cut)for unconverted and converted photons separately.

In order to further investigate the large discrepancy between the reco efficiencies of converted photons, we further divide the converted photon reco efficiency as reco conv and reco unconv reconstruction efficiencies showed in Figure 8. The reco unconverted efficiency(wrt true converted) in DPD is 16% while for xAOD it is 37%. The reco converted efficiency(wrt true converted) is 74% in DPD but for xAOD it is only 40%.

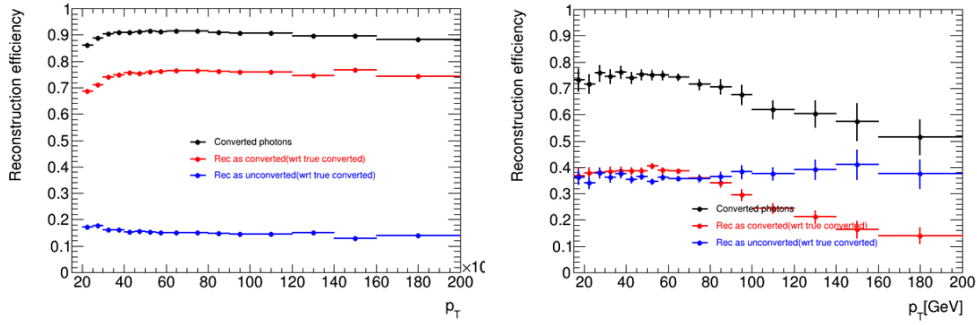


Figure 8: Photon reconstruction efficiencies as a function of true  $p_T$ (with acceptance cut) for converted ,reco conv(wrt ture converted) and reco unconv(wrt ture converted) photons separately.

These results are summarized in the Table:

Table 1:

Efficiency(%)	DPD	xAOD
Converted	90	77
$C \Rightarrow C$	74	40
$C \Rightarrow U$	16	37

## 2.2 The performance of the single photon sample @ xAOD

For the Higgs decays to diphoton sample, there are more than one photons in one event. If we want to perform more detailed check, we had better turn to singlephoton sample which comes from the sample release and tag number as the Higgs sample in xAOD for help. In this part, we try to separate the different conversion types, separate the detector regions, separate the different photon reconstruction processes and we perform the preliminary reconstruction quality check.

### 2.2.1 Separate the conversion type

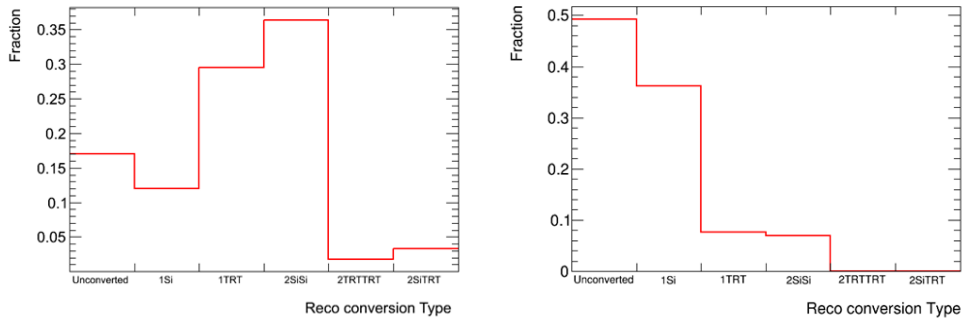


Figure 9: Reconstruction type for truth converted photons

Figure 9 shows the different reconstruction type for truth converted photons for DPD and xAOD singlephoton sample, nearly no 2TRTTTRT and 2SiTRT photons in xAOD are found, and the distribution are very different.

The reco efficiencies for different type of reco photons(wrt ture converted photons) are shown in Figure 10, for 2-track conversion , the efficiency in DPD is 34% while the efficiency in xAOD is 7%.



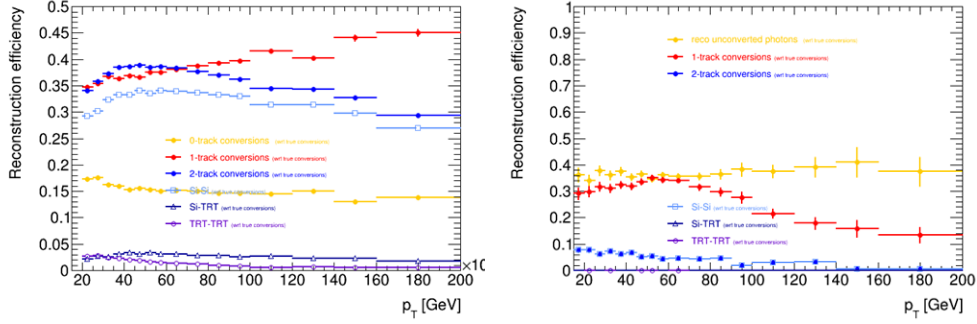


Figure 10: Photon reconstruction efficiencies as a function of true  $p_T$ (with acceptance cut) for different reco types

## 2.2.2 Separate the detector region

As it is shown in last section, we have found the large discrepancy between some reco efficiencies, then we like to figure out which detector leads to the high mis efficiency. In this section, we further divide the reco efficiency as a function of pixel detector radius [50,90],[90,123], SCT detector radius [290,380], [380,520], TRT detector radius [550,800], [800,1090](mm) in Figure 11

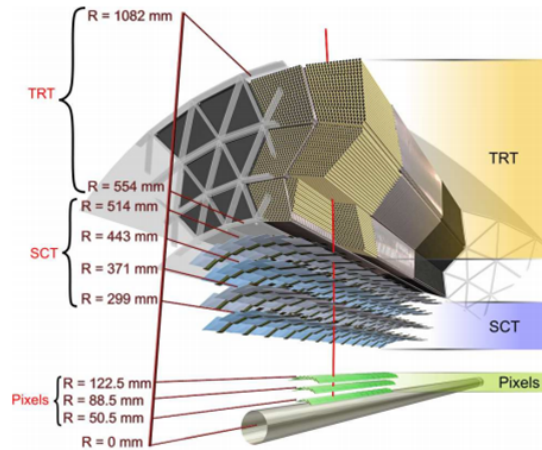


Figure 11: The Inner Detector overview

The truth converted photons distribution are shown in Figure 12 as a function of the detector radius. The truth converted photons fraction dominates in [600,800](TRT) region.

The truth converted photons reco efficiency are also shown as a function of the detector radius, it is clear that the discrepancy between the DPD and xAOD dominates in [550,800] region is large in Figure 13, there must be something wrong with the TRT subdetector

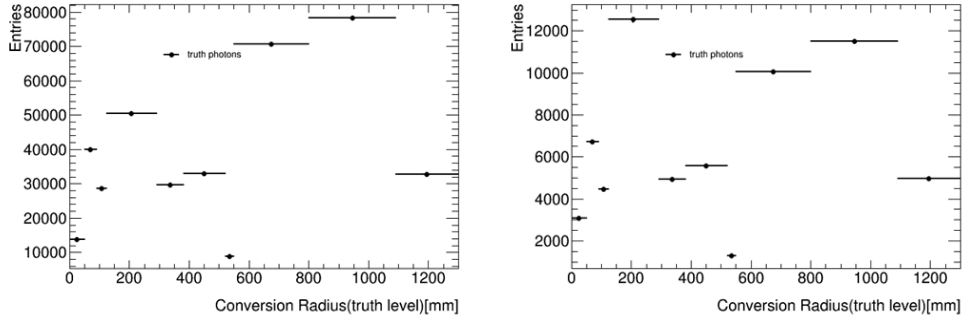


Figure 12: The truth converted photon distribution as a function of radius

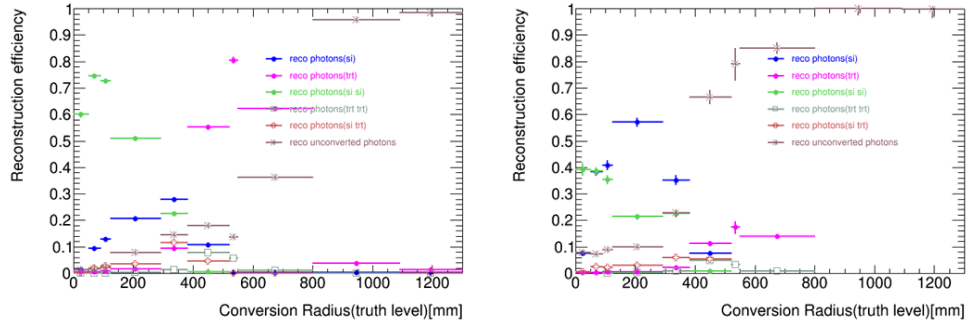


Figure 13: Photon reconstruction efficiencies as a function of true conversion radius for different reco types

### 2.2.3 Separate the reconstruction process

In this part we try to further figure out the issue causing the large discrepancy in TRT subdetector, so the study of the reconstruction process is performed[1][4].

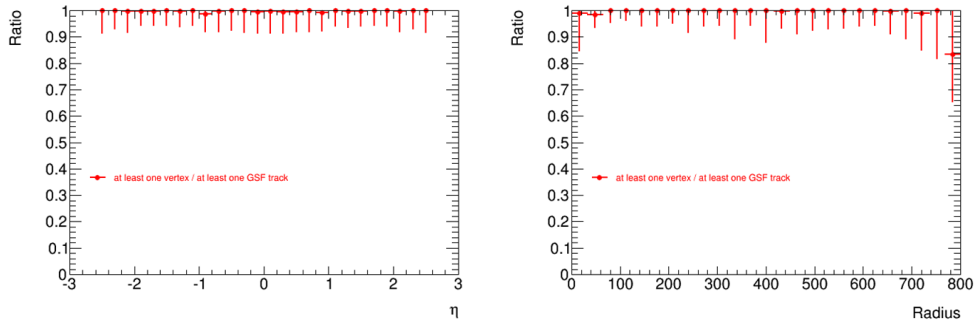


Figure 14: The ratios as a function of truth  $\eta$  and radius

In the Figure 14, the ratio of the number of photons and at least one vertex divided by the number of photons and at least one GSF track are shown, it is clear from this plots that from the photons and at least one GSF track, we can reconstruct the vertex very well.

We check the ratio of number of one converted photons divide by the number of photons and at least one GSF vertex in Figure 15, from this plot, it is obvious that something is wrong with the TRT region for the sharply drop in this region. This is because the vertex-cluster bug in the TRT region, the vertices are there but not reconstructed as converted photons.

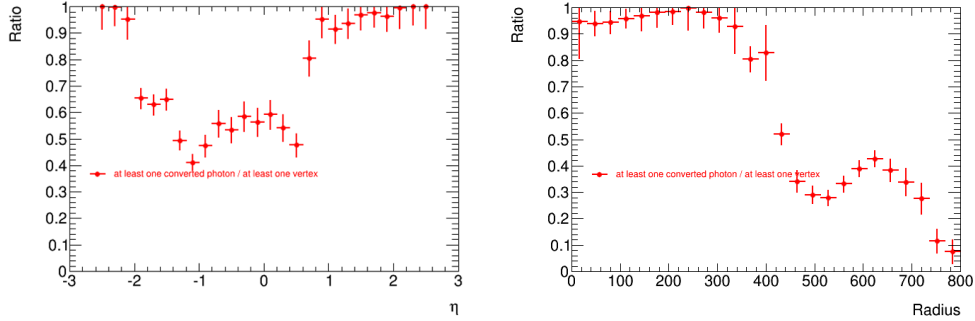


Figure 15: The ratios as a function of truth  $\eta$  and radius

we further divide the plots as conversion radius less and more than 400 mm shown in Figure 16

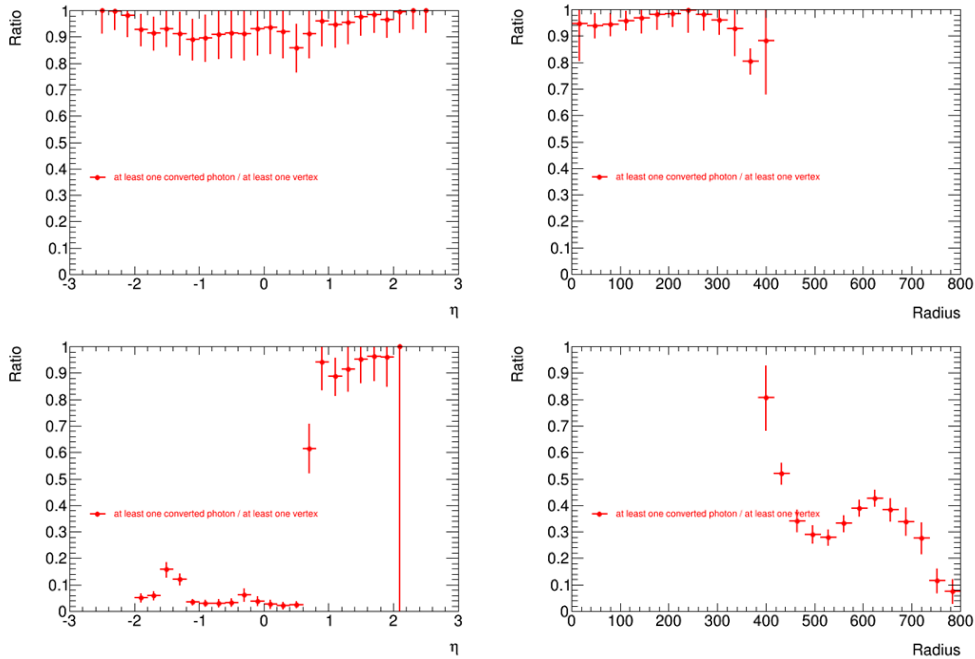


Figure 16: The ratios as a function of truth  $\eta$  and radius, top two plots show the radius less than 200mm

## 2.3 Latest xAOD reco efficiency results

In the last part in this work report, we have found the vertex-cluster match bug in the reconstruction process, after we fix the bug and show the mis-efficiency of truth converted reco as unconverted photons decreasing from 37% to 17% in Figure 17, it is a great contribution to the photon reconstruction of the ATLAS.

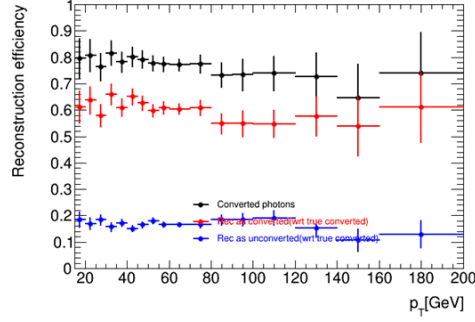


Figure 17: Photon reconstruction efficiencies as a function of true  $p_T$  (with acceptance cut) based on fixed xAOD sample

the latest reco efficiency results are shown in Figure 18:

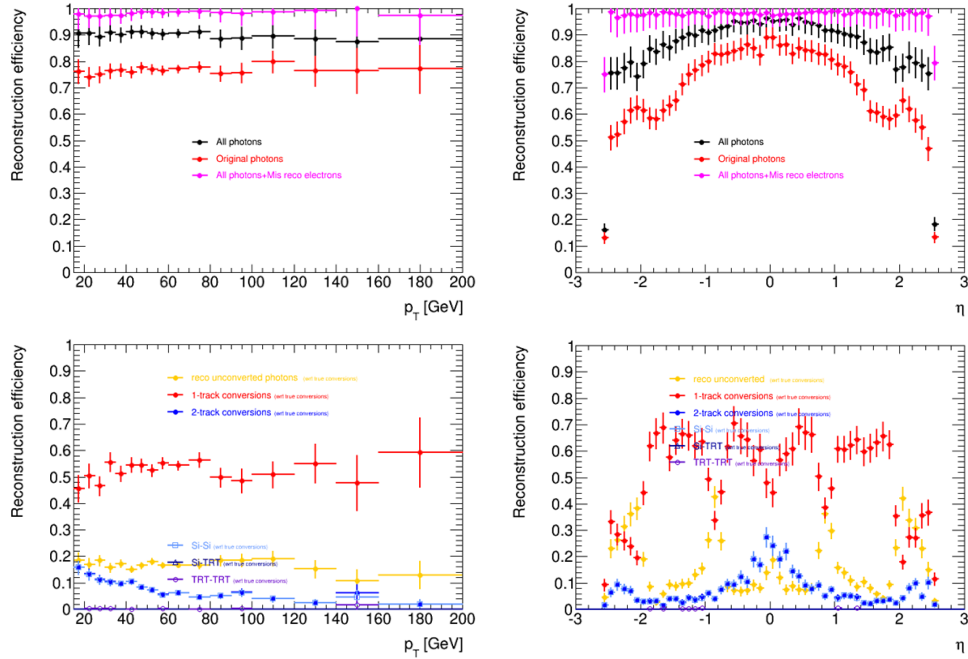


Figure 18: Photon reconstruction efficiencies based on fixed xAOD sample

In the end, summary table of the results from DPD and xAODs is given:

Table 2:

Reco Eff(%)	DPD	xAOD(19.1.1.1)	Latest xAOD
All photons	96	89	91
Original photons	59	79	77
Unconverted photons	100	98	99
Converted photons	90	77	80
Unconverted photons(wrt true converted)	16	37	17
1-track conversion(wrt ture converted)	40	33	53
2-track conversion(wrt ture converted)	34	7	10
2-sisi conversion(wrt ture converted)	32	7	10
2-sitrt conversion(wrt ture converted)	1.5	0	0
2-trttrt conversion(wrt ture converted)	0.5	0	0
Unconv fraction(truth level)	62	58	60
Unconv fraction(reco level)	68	83	73

### 3 Conclusions

This work report presents the photon reconstruction efficiency results based on xAOD. The comparison between the reco efficiencies from DPD and xAOD is shown and large discrepancy is found. Higgs decay to diphoton sample and singlephoton sample are used to hunt down the issues. After lots of work and careful check the reconstruction process, we have found and fixed a vertex-cluster bug in TRT region which decreases the mis efficiency from 37% to 17%. As the discrepancy between the 2-track conversion efficiency still exists, the further check is on going.

### 4 Acknowledgements

I would like to thank my supervisor Yanping HUANG for her consistent help and all the support from Deutsches Elektronen-Synchrotron(DESY) to this summer student program greatly.

## References

- [1] Expected photon performance in the ATLAS experiment, ATL-PHYS-PUB-2011-007 *The ATLAS Collaboration*
- [2] Reconstruction of Photon Conversions, ATL-PHYS-PUB-2009-006 *The ATLAS Collaboration*
- [3] Photon Conversions at  $\sqrt{S}=900\text{GeV}$  measured with the ATLAS detector, ATLAS-CONF-2010-007 *The ATLAS Collaboration*
- [4] Signal studies for  $H \rightarrow \gamma\gamma$ -8TeV, ATL-COM-PHYS-2012-755 *The ATLAS Collaboration*